ALEXIS-the Six Year Telescope Flight Experience

Diane Roussel-Dupr , Jeffrey J. Bloch, Elsa M. Johnson, and James Theiler

Los Alamos National Laboratory, Los Alamos, NM 87545

ABSTRACT

The Array of Low Energy X-ray Imaging Sensors (ALEXIS) satellite was launched from the 4th flight of the Pegasus booster on 25 April, 1993 into an 800 km, 70 degree inclination orbit. After an initial launch difficulty, the satellite was successfully recovered and is still producing 100 MB of mission data per day. ALEXIS, still going strong in its sixth year, was originally designed to be a high risk, single string, Smaller-Faster-Cheaper satellite, with a 1-year nominal and a 3-year design limit. This paper will discuss the on-orbit detector performance including microchannel plate operation, pre- and post-flight calibration efforts, observed backgrounds and impacts of flying in a high radiation environment.

Keywords: ALEXIS, EUV detectors, flight performance, ultraviolet, microchannel plates, astronomy, all sky monitor

1. INTRODUCTION

ALEXIS is one of the first modern, sophisticated, miniature satellites, and as such offers a lesson in miniature satellite design and development[1]. The ALEXIS satellite and experiments were funded by the Department Of Energy (DOE) as a technology demonstration mission, and was built as a collaboration between Los Alamos and Sandia National Laboratories (LANL, SNL), and UC Berkeley/Space Sciences Laboratory/ (UCB/SSL). The ALEXIS project was developed as a small skunk-work project headed by LANL. The custom, low cost, miniature spacecraft bus was built by AeroAstro, Inc., who also designed the original version of the groundstation. The ALEXIS satellite was launch-ready 3 years after its preliminary design review[2]. The Air Force Space Test Program launched ALEXIS using a Pegasus air-launched booster into a 70^{o} inclination, 400 x 450 nautical mile orbit on April 25, 1993. This was the fourth usage of this unique launch vehicle. The ALEXIS satellite is spin stabilized rotating once every 50 seconds. ALEXIS is controlled from the ALEXIS Satellite Operations Center (SOC) located at Los Alamos National Laboratory.

ALEXIS experienced a serious mechanical anomaly during launch but, after the initial recovery effort, this has only mildly compromised the performance, thanks to the dedication of the operations team. A broken solar paddle bracket during launch resulted in a failed magnetometer, which is mounted on the paddle. Because the automatic attitude control system required a working magnetometer, it could not function correctly to point the satellite at the Sun. Thus, currently, the orientation of the spin axis of the satellite is maintained by ground command. A detailed review of the launch, rescue mission and initial flight has been presented elsewhere[3,4].

In a 113-kg package, ALEXIS includes a six-telescope ultrasoft X-ray array (the ALEXIS experiment)[5,6] operating in narrow bands centered on 66, 71, and 93 eV (186, 172, and 130 Angstroms), a broad-band VHF receiver and digitizer (BLACKBEARD) both built by Los Alamos National Laboratory, a digital processing unit (DPU) built by Sandia National Laboratory, and a service bus (spacecraft) built by AeroAstro, Inc. A major objective of the project was to develop the capability at Los Alamos to design, construct, integrate, launch, and fly capable but cost-effective small satellites. Besides demonstrating new technical capabilities, the experiments are performing state-of-the-art measurements relevant to astrophysics and ionospheric physics.

The complement of six ALEXIS telescopes weighs 45 kg, draws 45 watts, and on average produces 10 kilobits/second of data. Position and time of arrival are recorded for each event. ALEXIS is always in a survey-monitor mode, with no individual source pointings. It is well suited for simultaneous observations with ground-based observers who prefer to observe sources at opposition because most sources in the anti-Sun hemisphere are routinely observed and archived. ALEXIS is autonomously tracked and controlled from a single small ground station located at Los Alamos utilizing a 1.8 meter tracking dish. Details of the operations have been presented by Roussel-Dupr [7,8]. Between ground station passes, data are stored in an on-board solid state memory with a capacity of 78 Megabytes.

The ALEXIS experiment, with its wide fields-of-view and narrow well-defined wavelength bands, complements the scanners on NASA's Extreme Ultraviolet Explorer (EUVE) and the ROSAT EUV Wide Field Camera (WFC), which are sensitive,

narrow field-of-view, broad-band survey experiments. ALEXIS' results also highly complement the data from EUVE's spectroscopy instrument due to the wavelength coverage overlap between the two experiments. ALEXIS' scientific goals are to: 1) map the diffuse background in three emission line bands with the highest angular resolution to date, 2) perform a narrow-band survey of point sources, 3) search for transient phenomena in the ultrasoft X-ray band, and 4) provide synoptic monitoring of variable ultrasoft X-ray sources such as cataclysmic variables and flare stars. Unlike other ultrasoft X-ray experiments, the 66 and 71 eV ALEXIS bandpasses are tuned to the Fe IX-XII emission line complex. This set of emission lines is characteristic of million degree plasmas which exist in the coronae of stars and which are thought to fill a large fraction of interstellar space around the sun, creating the soft X-ray background. While the maximum effective areas are small compared to other instruments such as EUVE or WFC (which have peak effective areas of several cm^2), ALEXIS has quite comparable area-solid angle response curves, which is the true figure of merit for sky survey experiments. The difference is that each ALEXIS telescope has a 33^o field-of-view, whereas EUVE or WFC have field-of-views of only a few degrees. As a result, ALEXIS can also excel in diffuse background studies, where large area-solid angle products are needed.

This paper will discuss the on-orbit detector performance including microchannel plate operation, pre- and post-flight calibration efforts, observed backgrounds and impacts of flying in a high radiation environment based upon 6+ years flight experience.

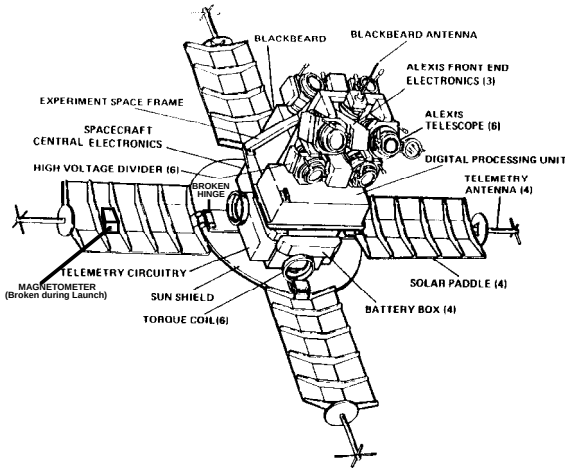

Figure 1: Schematic diagram of ALEXIS.

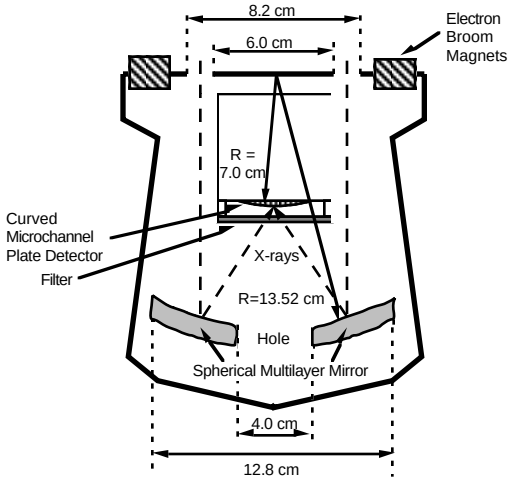

Figure 2: Cross-section of an ALEXIS telescope.

2. ALEXIS TELESCOPES

The ALEXIS telescope system is comprised of a Data Processing Unit (DPU), which provides the switched and conditioned low voltage power and high voltage power for the ALEXIS telescopes, command decoding, distribution and all onboard data processing, front end electronics (FEE) which does the pulse digitizing and initial processing, and the telescopes containing mirrors, filters and microchannel plate detectors. Details of the telescope design, calibration and performance have been previously reported by Bloch[5,6]. On orbit telescope performance has been presented previously by Bloch[9].

Table 1. ALEXIS Telescope Filter and Photocathode Characteristics and Telescope Pointing

Telescope ID	Filter Type	Photocathode	Bandpass Center	Center FOV degrees from spin axis
1A	Lexan/Titanium/Boron	MgF_2	93 eV (130 Angstroms)	88
1B	Aluminum(Silicon)/Carbon	NaBr	71 eV (172 Angstroms)	88
2A	Lexan/Titanium/Boron	MgF_2	93 eV (130 Angstroms)	56
2B	Aluminum(Silicon)/Carbon	NaBr	66 eV (186 Angstroms)	56
3A	Aluminum(Silicon)/Carbon	NaBr	71 eV (172 Angstroms)	28
3B	Aluminum(Silicon)/Carbon	NaBr	66 eV (186 Angstroms)	28

2.1. Telescope Overview

The ALEXIS instrument consists of six EUV telescopes are arranged in three co-aligned pairs and cover three overlapping 33° fields-of-view. They were originally designed to scan the entire anti-solar hemisphere during each 50-second rotation of the satellite. Each telescope consists of electron rejecting magnets at the telescope aperture, a spherical mirror with a Mo-Si multilayer coating, a UV background-rejecting filter in front of a curved profile microchannel plate detector located at the telescope's prime focus, and image processing readout electronics (see Figure 2). Telescope characteristics and pointing vectors are summarized in Table 1. The on-axis geometric collecting area of each telescope is ¯25 cm^2, with spherical aberration limiting resolution to about 0.25° of the pre-flight x-ray throughput calibration data indicates that the peak on-axis effective collecting area for each telescope's response function ranges from 0.25 to 0.05 cm^2.

2.2. ALEXIS Mirrors

The ALEXIS metal multilayer mirrors were designed at Los Alamos[10] utilizing a computer code developed by J. Bloch based upon the solution method of Born and Wolf[11]. Optical constants used for Mo, Si, and C were adopted from Windt[12], Palik[13], and DESY[14], respectively. A Debye-Waller factor was used to estimate inter-layer roughness. Comprised of alternating layers of molybdenum and silicon, the mirrors are optimized to provide maximum reflectivity at angles from 11.5 ° to 17 ° off normal incidence and at energies of 66, 71, and 93 eV. Simultaneously, the mirrors use a "wavetrap[15]" to suppress reflectivity at 304 , where the extremely strong geocoronal line of He II causes severe background problems. Γ, the ratio of the Mo to the d-spacing, typically ranged from 0.3-0.38 for the main mirror to 0.15-0.2 for the wavetrap.

Low reflectivity at 304 is achieved by superposing two layer pairs that provide destructive interference with an effective 2d spacing of 152 . The Mo layers in this wavetrap must be very thin, about 10 each, in order to allow the shorter wavelengths desired for peak reflectivity to penetrate without significant attenuation. Because refraction changes the effective angle of passage through the wavetrap, a joint optimization between layer thickness in the deep layers and the wavetrap layers must be performed for each target peak wavelength. For the 186 mirror, the optimum design from substrate upward is 40 layer pairs, each 74 Si and 31 Mo, followed by 2 layer pairs, each 55 Si and 10 Mo. Calculations predict this design would have a peak reflectivity at 186 of 35% and a 304 reflectivity less than 10^{-5}.

The ALEXIS mirrors were fabricated on highly curved, large quartz blanks (diameter = 12.8 cm, radius of curvature = 13.52 cm) which had been polishes to a surface roughness of †2 rms at General Optics. Ovonyx, Inc. vacuum deposited via magnetron sputtering the metal multilayers in 1990 after an extensive joint development program to improve the d-spacing uniformity on severely curved surfaces[15]. To improve center-to-edge d-spacing uniformity, the optics were spun at 6 rps. At the time of deposition, flat witness mirrors, 4 cm diameter quartz flats, were placed in a hole in the center of the flight mirrors. Throughout the calibration and handling of the flight mirrors, these flat witness mirrors were been paired with the flight mirror to be used as contamination monitors as they could more easily be removed from the telescopes for periodic measurement.

During laboratory calibration, it was discovered that the mirror reflectivity at HeII 304 was degrading as a function of time. Mono-layer contamination was forming even with best efforts during handling. The source of the contamination was consistent as being carbon-like from the modeling effort and was later confirmed by ESCA measurements. Faced with the fact that if the contamination continued at the same rate the measured reflectivity at launch would be an unacceptable few x 10^{-2}, we developed a wavetrap recipe for the 66 and 71 eV mirrors. This new recipe was optimized such that was purposely too

Table 2: ALEXIS Mirror Reflectivity Properties

			Primary Reflectivity			
Mirror label	Energy	Wavetrap	Peak	Theoretical (no roughness)	304 Reflectivity as measured in 1992	Comments
xro4763	93 eV	Mo/Si	.6	.8	2-3 x 10^{-4}	2 sets of coatings
xro4770	93 eV	Mo/Si	.6	.8	2-3 x 10^{-4}	2 sets of coatings
xro5306	66 eV	C/Mo/Si	.32	.35	3 x 10^{-3}	at least 2 sets of coatings
xro5339	66 eV	C/Mo/Si	.28	.35	3 x 10^{-3}	at least 3 sets of coatings
xro5369	71 eV	C/Mo/Si	.35	.45	3 x 10^{-3}	at least 2 sets of coatings, dirty sputtering chamber

xro5371	71 eV	C/Mo/Si	.38	.45	3×10^{-3}	at least 2 sets of coatings, dirty sputtering chamber

thin when sputtered, but should grow to be nearly optimal at launch (or at least this was the hope). The filter on the 93 eV mirrors was thick enough that the wavetrap was in principle not needed and thus, these mirrors were flow without a wavetrap. The final flight recipe replaced the top layer of Mo with a "cap" of 15 of carbon allowing the C and contamination to effectively "replace" the top Mo layer. With this recipe, the initial wavetrap fabricated in 1991 was slightly better than no wavetrap but the wavetrap would improve as an estimated additional 15-30 of "carbon-like" contamination formed on the top of the mirror prior to launch in 1993. This, however, required that the mirrors be recoated as there were not enough spare mirror blanks to coat afresh. It proved feasible to deposit a second and in some cases a third multilayer structure over the original coating when the first results were not satisfactory. Some loss of uniformity (3-5%) was noted comparing the initial measurements to the final flight coatings that was attributed to increased interlayer roughness.

2.3. ALEXIS Microchannel Plate Detectors

The ALEXIS microchannel plate detectors are single photon imaging detectors and were produced and calibrated by UCB/SSL[17]. The detectors, designed to operate near 4500 V, contain two 46 mm diameter microchannel plates, each with 12.5 micron diameter channels. The channel length to diameter ratio is 120:1. The front plate has a 0^{o} channel bias, while the back plate has a 13^{o} bias angle. The top plate surface has a radius of curvature of 7 cm, while the bottom plate surface curvature radius is 6.8 cm.

The detector wedge and strip anode, made of fused quartz, has a plano/spherical shape with a 5.8 cm radius of curvature. The anode material is evaporated copper and has a pattern period of 1 mm. The diameter of the anode is 40 mm. A magnetic shield made of 410 stainless steel, 1.5 mm thick, surrounds the outside of the detector while the electric field between the microchannel plates is shaped by a semiconductive layer inside the ceramic body. The detectors intrinsic spatial resolution performance of 85 microns significantly oversamples the optical point spread function of the telescope.

The top surface of the microchannel plates has one of two photocathode coatings depending on the bandpass. 66, and 71 eV bandpass telescopes (1B, 2B, 3A, 3B) telescopes had NaBr as a photocathode. The 93 eV bandpass telescopes (1A, 2A) has MgF_2 as a photocathode. Because of the hydroscopic properties of the MgF_2, the detectors were either stored at vacuum or at dry N_2 before launch.

A unique feature incorporated into the ALEXIS detector design is a small circular aluminum mask (with a diameter of 0.564 cm) placed permanently over a small part of the front of the detector at the edge of the active area. The mask shields a section of the detector from any incident EUV radiation. Thus any events located within that area arise from intrinsic dark counts or high energy penetrating particles. The event rate in this area is used as an on-orbit monitor of high energy particle induced events. Calibrations with radioactive sources on the ground determined the relationship between particle induced events under the mask and over the rest of the detector. This kind of background monitoring is essential to remove the non-cosmic flux from the measurement of cosmic diffuse EUV emission.

After delivery to LANL, the detectors were installed in the telescope bodies and calibrated again as a system. During this second calibration, the detectors were run at several different voltages and a final set of "flight" voltages was determined based upon optimal detector performance.

The ALEXIS telescopes were launched at a near vacuum with the last pumping occurring 2.5 days before launch. The telescope bodies were not perfectly leak proof; pre-flight testing indicated that they either leaked or outgassed at 200-300 mTorr per day, therefore, there were expectations that there would be a small partial pressure in them at launch. The original

Table 3 ALEXIS Telescope Flight High Voltage History

	door open	first HV	HV at reduced setting	HV at full flight	Final Flight HV 1993	Final Flight HV 1995	Final Flight HV 1999
1A	8/7/93	9/3/93	9/3-11/93	9/11/93	4320	4320	4320
1B	8/7/93	9/3/93	9/3-11/93	9/11/93	4400	4400	4400
2A	7/25/93	7/31/93	7/31/93-8/9/93 9/1-11/93	9/11/93	4550	4550	4550
2B	7/25/93	7/31/93	7/31/93-8/9/93 9/1-11/93	9/11/93	4250	4300	4300

3A	7/22/93	7/27/93	7/31/93-8/9/93 9/1-11/93	9/11/93	4450	4600	4600
3B	8/31/93	9/5/93	9/6-11/93	9/11/93	4450	4700	4700

operations plan called for the detector doors to be opened one at a time, two per day starting on the fifth day after launch. The
primary concern was some residual outgassing of the spacecraft might contaminate the telescope mirrors and thus destroy the 304 anti-reflection coating. After the doors were opened, a two day wait would occur for the telescope bodies and especially the microchannel plates to outgas before HV would be turned on.

In actuality, due to the launch problems, the detector door opening did not start until 22 July, 1993 after initial contact and recovery with first HV operations starting on 27 July on one of the detectors. By this time, the satellite was well outgassed and any concerns about contamination of the mirrors was no longer an issue. For the most part, the door opening activities were straightforward with the doors opening on the first or second try except for telescope 3B, which eventually opened after repeated tries.

All telescopes when first turned on had high counts rates which gradually decreased over several days of operation at reduced HV, some more quickly than others. Telescopes 3A, 2A and 2B, the first telescopes to be turned on, were left at reduced HV settings for numerous days while the flight team acquired full understanding of what flight threshold settings to use to accommodate the large background. In the midst of this operation, contact with the spacecraft was lost between August 9-26, 1993 due to elevated temperatures on the transmitter board. Telescope pair 1 was allowed to outgas the longest before HV operations were commenced; it is interesting to note that these were the easiest to configure, but it is unknown whether or not it is due to the longer outgassing times. The telescope door˚open and HV on sequence is summarized in Table 3.

The detectors were brought up to flight voltage in steps to assure safe operations and the final flight settings were those determined in the laboratory pre-flight. Two of the detectors, however, were only stable at a slightly reduced flight voltage (50 V lower). Initially, one or two of the detectors, which were known to be problematic, would go into a self scrub mode, but lowering the voltage 500-1000 V for 1-3 days seemed to cure the problem. However, in mid-November, 1993, several of the detectors went into self scrub mode simultaneously, an effect that we later attributed to 1) the orbit was such that the detectors were operational during times of higher particle flux because they were turned on for long periods in the northern auroral zone which was in darkness and 2) the solar wind was greatly enhanced due to a well placed coronal hole which increased the number of particles in the auroral zones. After several weeks of running at lower voltage, we were able to regain normal operations of these detectors; however, it was determined to be necessary to lower flight voltage on two of the detectors by 50-100 V to assure stable operation. Decreasing the working voltage did not significantly affect the operation of these detectors. After 2 years of operations, however, we again increased the 3A and 3B voltages by 150-250 V to regain the lost detector gain which has been stable since that time. Since 1993, instances of detector self scrub occasionally have occurred (less than once or twice per year), but the frequency of occurrence has been decreasing as the detectors mature.

2.4. ALEXIS Filters

The ALEXIS detectors are limited to the 66 to 95 eV bandpass regime by the reflective properties of the mirrors as well as thin film filters supported on wire mesh in front of the detector. The filters were designed to reject the longer wavelength UV and EUV geocoronal radiation, which the detector photocathodes would detect and which would still reflect significantly off of the telescope, mirrors at normal incidence. Lyman Alpha, HeII 30.4 nm, and HeI 58.4 nm geocoronal radiation were of particular concern due to their intensity.

The filters were procured from Luxel Corporation. The 66 and 71˚eV ALEXIS telescopes are comprised of 1200 of aluminum and 600 of carbon while the filters for the 95 eV telescopes are comprised of 1500 of Lexan, 200 of titanium and 900 of boron. All the filters were deposited on a 70 lines per inch Nickel mesh (manufactured by Buckbee Mears) with a transmission of 82%. Each filter has a diameter of 46 mm. A detailed discussion of the flight performance of the ALEXIS filters are presented at this conference by Starin, et al, 1999[18].

Early in the mission, it was discovered that the filters were not optimized for daylight, earth looking operation. This, plus the unexpectedly large background, required a significant change to operation plans; instead of turning on the telescopes and leaving them on for all time, to assure the safety of the detectors as well as the electronics, command sequences were written to only turn on the detectors during the eclipse part of the orbit.

After first light through all telescopes, it was determined that one telescope (2A) had acquired three pinholes near the edge of the filter support ring which appeared as three small donut shapes in the detector image. Although it is not possible to now

use these portions of the detector for cosmic observations, the actual percentage of the total detector area is small, so it is only a minor impact to the observing program except for the effect on the count rate. Since the detector electronics is only capable of digitizing 200 counts per second, UV photons, which are detected due to the pinhole leaks, compete for the digitizable data budget, thus, reducing the number of EUV photons detected.

After the December, 1994 period of 100% sunlight illumination, first turn-on data showed that the filter for telescope 3A had developed pinhole leaks near the edge of the filter support ring. These new pinhole leaks in 3A were the first and only filter degradation since launch. The cause of the pinholes creation is still unknown. 3A runs the coolest due to the fact that it looks nearly along the spin axis which would seem to rule out thermal stress and it also sees less background due to RAM, so atomic oxygen erosion is unlikely. The best guess is that the pinholes were created due to thin film stress failure. Luckily, unlike TP2A, which has pinholes in the high gain region, the pinholes in TP3A are at the bottom of the low gain region and as such do not contribute a significant amount to the total count.

In addition to the above mentioned persistent pinhole filter leaks, additional weak UV leaks have been detected in the ALEXIS data which may be due to fabrication non-uniformities, micro-pinhole production or thin film surface crazing. The filters were designed to eliminate light from all but the brightest early type B stars. However, during the second and third year of the mission, it was noted in composite sky maps of a month or more that the brightest of these stars were detectable at a low level in one of the detectors. Detailed detector images have shown that only localized regions of the filter are responsible for the leak. Since that time, it appears that all filters have developed regions of enhanced B star detection. While not important for point source detection efforts, these regions of weakly leaking filters may be an issue for the EUV diffuse background studies.

2.5. Experiment Data Processing Unit

During the first 3 months of telescope operations, the operators were besieged daily by both hard (back into bootstrap mode) and soft resets of one or more of the four DPU's. The DPU'swould be tripped as the satellite crossed 1) the South Atlantic Anomaly (SAA), a region above the South Atlantic where satellites encounter a swarm of trapped charged particles, 2) the Auroral zones or 3) the polar cap regions. It was eventually determined that the resets were not due to a DPU problem, but rather due to the way Error Detection and Correction (EDAC) hardware interrupts were being handled in software. Every time a DPU memory error is detected an interrupt routine is called to correct and report the bit error. A fault in this routine would cause a processor reset. This fault was missed by software testing since Single Event Upsets (SEUs) are infrequent on the ground and the simulation method proved inadequate. A minor software poke corrected this fault which greatly simplified daily operations.

After this fix, other, more extensive fixes were required of the DPU code to accommodate the actual on-orbit performance of the ALEXIS experiment. The primary difficulty in collecting science data was due to the fact that during a single satellite spin (50 sec), the count rate could vary between 20-20,000 counts/sec. Count rates in excess of 20,000 counts/sec trigger a software safing mode intended to shut down the HV supply for up to 2 minutes at a time during times of high count rates like in the SAA which for non-SAA resulted in significant loss of data. A software fix to "throttle" down the HV level by 300 volts based on count rates now allows us to collect data continuously over a spin of the satellite. A second major difficulty due to the background is that in order to keep the detectors healthy, the telescopes are only turned on during times of eclipse. This requires daily uploads of stored command of more than 280 commands to each telescope CPU to turn on the electronics, configure for observations, make the observations and turn off at the end of each orbital eclipse. Originally conceived as a turn-on and stay-on experiment, the originally limited number (200) of allowable stored commands has recently been increased to accommodate greater than 48 hour operations between command uploads which was required as automated operations were brought on line. Thus, features that we thought would be "Nice-to-Have" before launch became essential due to the current operational constraints.

Due to the extensiveness of the modifications to the DPU code and the inability to fully test every possible scenario, especially the extreme high and low count rates per spin, the only real test of the software was to upload it to the satellite after it passes initial ground testing. Several iterations of the code were required. Although initially, the first version of code was programmed into the 64K-16 bit word EEPROM, later, to minimize the number of times we reprogrammed the EEPROM, new code was later first programmed into the on-board, 256Kwords of EDAC RAM and then transferred to the EEPROM when it appeared to be working correctly. Although care was taken to assure that no code was uploaded in regions of high particle background like the northern auroral region, for unknown reasons, reprogramming often times required uploading the same files one to three times before a successful upload was obtained. Telescope pair number 2 was the least efficient of the three pairs of telescopes and thus, chosen for this risky operation. In the end, eight to ten versions of code were uploaded to DPU2 before all of the changes were working optimally of which five versions were uploaded into

EEPROM. Only one or two additional code uploads were required for DPU s 1 & 3. After several years of use, the code appears to be working very well, and has greatly improved the amount and quality of data from what was originally being collected.

One major concern with regards to the uploading of new DPU code was the determination that the EEPROMS have a finite programmable lifetime of 1-2 years due to radiation damage. These concerns were based upon radiation testing by Sandia National Laboratory that determined that after a certain level of radiation exposure, the voltage pumps become damaged on the chips which precludes additional re-programming. Given ALEXIS' orbit and a worst case analysis for the radiation exposure for the EEPROMS, it was estimated that the EEPROMS could be reprogrammed for up to 18 months (J. Griffee, SNL, private communication). Therefore, there was a concerted effort to complete all DPU modifications before time ran out. Later in the mission, however, a portion of dual ported ram between the spacecraft and the science experiments failed after 4.5 years on orbit. A patch was successfully programmed into the spacecraft EEPROMS in August, 1998 after more than 5 years of radiation exposure indicating that the total radiation dose might not have been as high as estimated due to the fact that much of the mission occurred during solar minimum.

3. CALIBRATION

3.1. Ground Calibration and Throughput Calculations

The Space and Remote Sensing Sciences Group at Los Alamos National Laboratory built a calibration laboratory to provide reflectance measurements and calibrations for the ALEXIS satellite project. The calibration laboratory, the primary component of which is an ultraviolet/soft-x-ray reflectometer, is in a class 100 clean room, along with a telescope gimbal system, a vacuum storage system, and an optical alignment table. The ALEXIS telescopes were assembled in the laboratory and the reflectometer was used to evaluate sample multilayer coatings for the telescope mirrors, measure the mirrors, and calibrate the telescopes. The reflectometer includes a goniometer in a vacuum chamber and a monochromator with a Penning discharge ultraviolet (UV) source (a commercially available item from Berkeley Photonics) which covers the wavelength range from 130 to 1550 . Software running on a Sun SPARCstation performs the data acquisition and analysis.

3.1.1. Background Testing

Long duration measurements of non-light stimulated detectors were made to study the uniformity and amount the detector dark noise counts. These test showed that on average, the summed count rate for each detector was of order 5-8 counts/sec. Co60 radioactive sources were used during these non-light stimulated tests to help characterize the pulse height and spatial distribution of penetrating particles.

3.1.2. Spatial Imaging Linearity Calibrations

Once the mirror and detector were installed into the telescope body, the unit (without the filter) was placed in the calibration chamber. This setup was used to further check the focus of the telescope as well as map out the relationship between X-Y location of events on the detector and the direction of the incoming rays. The gimbals on which the telescope was mounted were manipulated by two computer controlled motors. This entire test was automated and controlled by a SUN workstation.

The data collected with these calibration sequences were analyzed to produce arrays of telescope coordinate unit direction vectors representing the look direction in the telescope FOV for each active detector pixel. To produce these arrays, the image of the collimated UV source on the detector for each gimbal pointing was centroided. The resulting list of gimbal angles and detector X-Y locations was used in a two dimensional spline fit process to produce the final arrays of vectors for all active detector pixels.

3.1.3. Pencil Beam Throughput Calibrations

The final tests for telescope system throughput were performed by an EUV pencil beam . After the spatial mapping calibration test was completed, the flight filter was placed on the detector and the unit re-assembled. The telescope was then placed back in the vacuum chamber with the gimbal mount, and then the vacuum chamber was placed on a port of the LANL EUV reflectometry system. A monochromatic pencil beam of calibrated intensity was then directed into the entrance aperture of the telescope. The telescope was gimbaled to different angles so that the pencil beam traversed different paths through the telescope. The resulting output from the telescope was compared with calculations to determine the final model of telescope

performance as a function of wavelength. Using the pencil beam data for telescope 1B where each pointing simulates a star position and a pseudo satellite ephemeris, Figure 3 shows the gimbal positions as projected on the sky and compares this to an actual image of HZ 43. This plot clearly shows the detector spatial linearity and the 0.25 degree detector resolution.

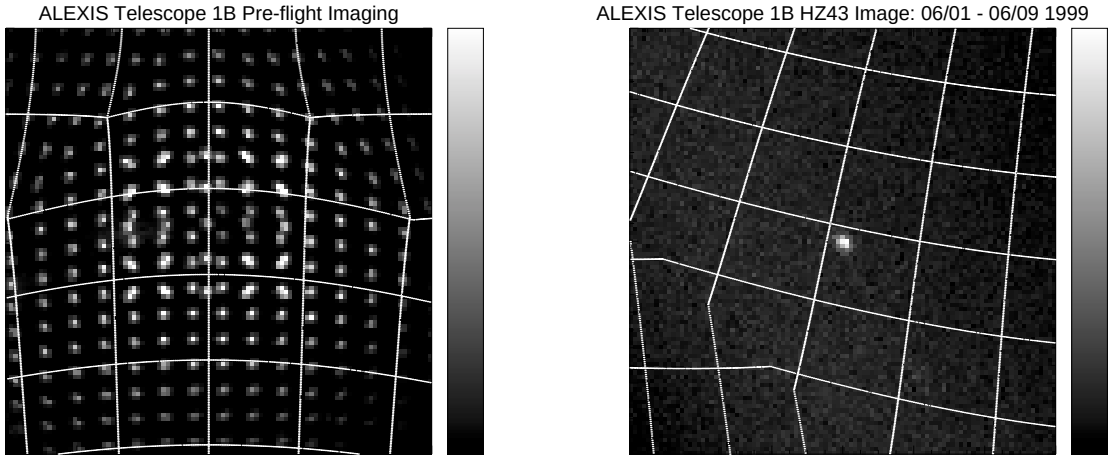

Figure 3: Comparison of pre-flight imaging performance with in-flight point source images for ALEXIS telescope 1B. Both the right and left images were processed with the full ALEXIS sky mapping data processing pipeline. The image on the left was created from data collected during ground calibration in which a parallel beam of UV light was aimed at the aperture while the telescope was rotated on a two axis gimbal to different orientations, 1.0 - 1.5 degrees apart. A fake satellite aspect was created to process these data in which the satellite stays in a fixed orientation. The image on the right is a summation of raw sky map images of the region around the bright EUV source HZ 43 collected between June 1, 1999 and June 9, 1999 while the satellite was spining with a period of approximately 50 seconds. In both images the pixel size is 0.25 degrees, and the Quadrilaterilized Spherical Cube map projection is used for both images. The grid lines are 5 degrees apart.

3.1.4. End-to-End Simulation

A computer model has been constructed to include the geometrical optics and the angular and wavelength responses of the components of this system for evaluation of the total response of the system. This model has strived to include realistic models of all components of the telescope system. Initially before laboratory measurements were made, simplified theoretical models were used for each component, but these models has gradually been replaced by real measurements. Unfortunately, this end-to-end simulation was not completed prior to launch. As with all complex systems being developed on a tight timeline, it was later determined that not all measurements were optimally made. Post-launch, there has been a concerted effort to systematically go through each component of the model to assure their accuracy. In doing so, interpretation of the original calibration data has required extensive effort as discrepancies between the model and the flight data have surfaced. This work is still in work and will be discussed in a future paper by Bloch, et al[19].

3.2. On Orbit Calibration and Throughput Calculations

Pre-flight, there was a concern that the ALEXIS mirror response would change due to 1) the ALEXIS mirrors being significantly impacted by atomic oxygen which would change the reflective properties even though the top mirror surfaces

Table 4: ALEXIS Pre-Flight and Observed Count Rate for HZ 43*

Telescope	Pre-flight estimates c/s	Observed c/s 1994	Observed c/s 1995	Observed c/s 1999	Comment
1A	0.12		0.063+/-0.015 c/s	0.075+/-0.015 c/s	Discrepancy due to mirror response much narrower than initially predicted
1B	0.49	0.46 +/-0.05 c/s	0.49+/-0.05 c/s	0.43+/-0.05 c/s	

3A	0.18		0.26+/-0.03 c/s		
3B	0.13		0.18 +/-0.02 c/s		

*count rate averages determined using only center 5 degree of detector

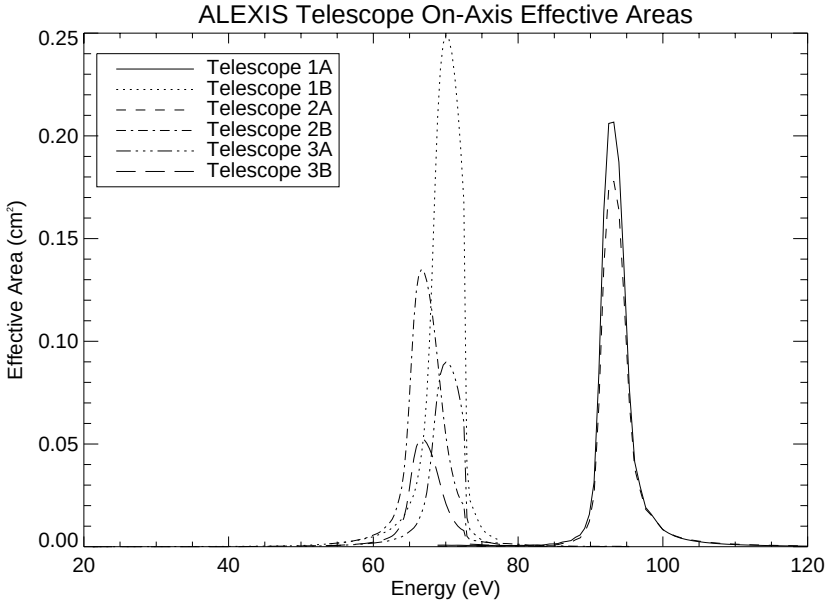

Figure 4: The ALEXIS telescope pre-flight on-axis response function.

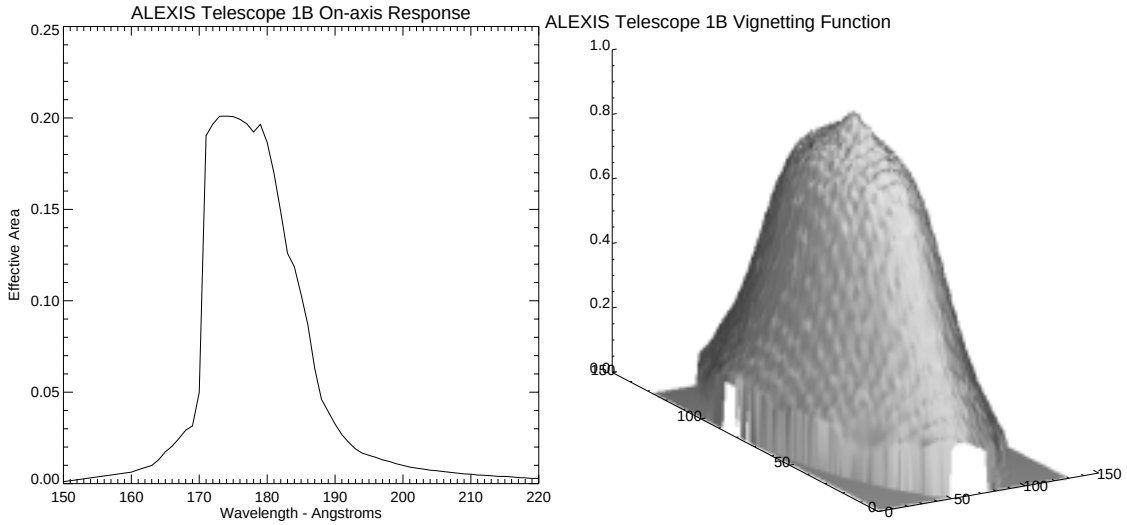

Figure 5: The plot on the left indicates our best post-flight effective area verses wavelength curve (on axis) for ALEXIS telescope 1B. The shaded surface plot on the right is our best post flight representation of the EUV telescope vignetting function for telescope 1B over the entire field of view. The effective area curve resulted from a detailed analysis involving the reconciling of a detailed physics model of the telescope with monochromatic pencil beam calibrations taken before flight. The vignetting function was derived from this physics model and adjustments to it made from flight data on the relative response of the telescope to the strong EUV point source HZ43.

were designed with some oxidation in mind and 2) the long delay in opening the ALEXIS doors therefore subjecting the MCP's to a small partial pressure of gas might have significantly changed the detector sensitivity. The only way to determine whether or not there is any degradation on orbit of any of the telescope components is to monitor a calibrated cosmic source and check to see if there has been any change in the total throughput of the system since final calibration in the laboratory. To this end, the brightest, constant cosmic, non-solar system source, HZ 43, has been observed by the ALEXIS telescopes for long periods of time twice a year in all three telescope pairs. The source count rate has remained constant and is consistent with pre-flight estimates as will be discussed below.

The HZ 43 count rate has also been compared to the pre-flight estimates. Unfortunately, only telescope 1B was fully calibrated pre-flight . The other telescopes were partially calibrated due to the short time allowance with the hope that 1B results could be used to aid the calibration of the other telescopes. Thus, although the agreement between pre- and post-flight counts rates for 1B is quite good, there are some discrepancies for the other telescopes. Table 4 presents some of the observed HZ 43 count rate data. Note that not all telescopes observed HZ 43 near the center of the FOV and are, thus, not included in this table. This data uses the pre-flight response and vignetting functions, which are known to have problems near the detector edges. Therefore, to minimize these known features, Table 4 only contains averages of detections within the central 5^{o} of each of the detectors. Although there are some differences between pre-flight and on-orbit measurements, the important point to note is that the source count rates have remained essentially constant implying the telescopes as a system are not degrading or changing with time.

Figure 4 shows the pre-flight detector on-axis response functions. The left hand panel in Figure 5 shows the most recently derived on-axis response function for telescope 1B. The pre-flight curves are different from the flight currently being derived due to the differences between the desired and as fabricated mirror coatings. The final mirror coatings have a slightly different as fabricated d-spacing as well as interlayer roughness that effects the actual shape of these curves. However, these curves have been qualitatively verified by observations of HZ 43 on-orbit at detector center. HZ 43, is ideal for this quick check because it is a constant bright EUV source that has an effectively flat spectral emission across the ALEXIS bandpasses. Other sources like G191-B2B contribute mostly at longer wavelengths where uncertainties in details of the wings of the response function can significantly affect the total source count rate. The on-axis effective area curves for ALEXIS are quite comparable to the effective area curves for the spectrometer instruments on EUVE. Thus any transient source detected with ALEXIS will only require comparable effective exposure times with the EUVE spectrometers to measure the source spectrum.

One of the principal unknowns in the system is the exact nature of the vignetting function. Preliminary studies of HZ 43 in all telescopes as a function of field of view angle have shown that beyond 8 degrees from the center of the detector that the source count rate starts to diverge significantly compared to the count rate at the center of the detector for telescopes 2B, 3A and 3B. The quantum efficiency of a microchannel plate detector is not only dependent on wavelength, but also the angle between the incoming ray and the axis of the microchannel plate pores. Because the microchannel plate pores are parallel to the optical axis, this distribution also reflects the way rays traverse the filter in front of the detector. The reflectivity of the mirror at a given wavelength is also a strong function of the angle with which the ray reflects off of the mirror due to the nature of the interference character of the multilayer that covers the mirror surface. The ALEXIS throughput calculation requires a complex folding of these 2 features in addition to spatial uniformity of the mirrors. The resultant vignetting function for each telescope is a separate, very steep and complex function that is difficult to predict based upon ground test data alone. The right hand side panel of Figure 5 shows the most recently derived vignetting function for telescope 1B. HZ 43 observations at various positions on the detector are currently being used to derive a flat field function for each of the telescopes. Errors in the vignetting function will lead to errors in the estimates of the effective exposure and thus, the source count rates. Consequently, the recent effort has been focused on vignetting function determination.

4. ON ORBIT PERFORMANCE

Prior to launch, the experiment team had expected that the ALEXIS telescopes would be highly robust to a variety of on-orbit non-cosmic backgrounds that have been problematic for other x-ray and EUV telescope systems. The fact that the design uses normal incidence, rather than grazing incidence mirrors means that any charged or neutral particles have to bounce at a large angle off of the mirror surface (thereby losing a lot of energy) in order to travel towards the detector. After that the particle would still have to travel through the filter material before reaching the microchannel plate. High energy particles, which might fluoresce the mirror and generate a photon background for the detector were to be rejected by an octopole magnet assembly at the aperture of the telescope. These magnets were designed to reject electrons of up to 0.5 MeV. The filters were carefully optimized to reject FUV radiation present on orbit. Count rates outside of the auroral zones and South Atlantic Anomaly were expected to range from 10 to 50 counts per second over the entire telescope field-of-view depending on the telescope and the assumptions about the spectrum of the soft x-ray background. He II 304 radiation from the geocorona would cause ~1 count/second/Rayleigh in the telescopes with Aluminum/Carbon filters (typical intensity values for He II 304 range from 0 to 12 Rayleighs), and not affect the telescopes with Lexan/Boron/Titanium filters at all. In the calibration laboratory, all detectors had background rates between 5 and 8 counts/second due to residual radioactivity in the microchannel plate glass. Penetrating radiation on orbit was expected to add an additional ~5 counts/second of background over the entire field-of-view.

4.1. Anomalous Background

At first light, the ALEXIS background was observed to be much brighter than predicted pre-flight, as much as 20,000 counts per second instead of 10-50 counts per sec predicted pre-flight. In addition to being much brighter than expected, the count rate varied rapidly between 10-20,000 counts per second during each spin of the satellite. Originally, before the first attitude solution was derived, the source of the background was thought to be the bright earth in the ALEXIS bandpasses as the

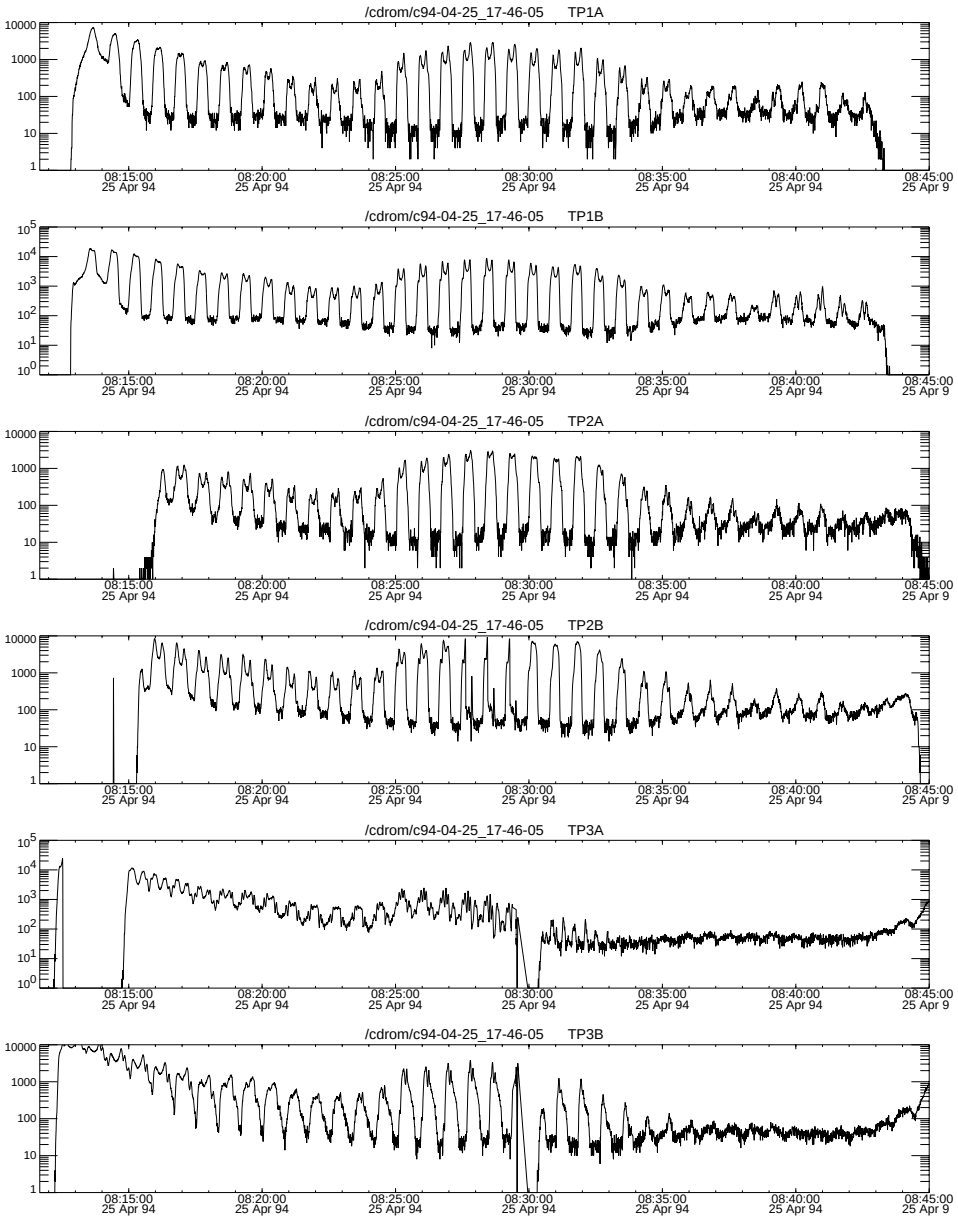

Figure. 6: ALEXIS telescope count rate during one night time orbit during 25 April, 1994. Note the approximately constant lower envelope of the counts except during the first 5 minutes that are contaminated by auroral penetrating particles and the spin modulated extremes from 10-20,000 c/s and the strong central enhanced envelope that correlates with the Earth's equator. The center 3 revolutions of telescope 2B show the effect of "throttle", the condition when the count rate exceeds 20,000 c/s and the onboard software lowers the detector high voltage by 600 V. The lack of counts at 8:30 for TB3 shows the effect of a reset where the FEE was unable to keep up with a rapid change in the digitization rate causing a 50 second loss of data.

background was modulated with the spin period and present for about 50% of the spin period. However, this was eventually proven to be an incorrect assessment when the first attitude solutions became available. A detailed summary of the background as it is understood to-date has been presented by Bloch et al[9] and Roussel-Dupr et al.[20].

Figure 6 shows detector count rates as a function of time for all six ALEXIS telescopes for a portion of one orbit's data that was collected April 25, 1994. The character of these plots is typical for most ALEXIS telescope data. Note the large oscillations that occur at the spin period of the satellite. This data comes from pulse counting rate scalars in the telescope front end electronics whose accumulations are reported in the telemetry stream every 0.5 seconds. The electronics can only digitize events at rates below 200 counts/second per telescope, so no individual event information is available at rates higher than 200 counts/second per telescope.

Due to the varied character of the background, it appears that the background has several different components:

1) A hemispherical enhancement, modulated with spin period, is observed simultaneously in all 6 telescopes throughout a major portion of the eclipse part of the orbit. The enhancement covers approximately half the sky, thus, reducing the duty cycle to 50% of pre-flight estimates.

2) A broad, bell shaped, spin modulated enhancement of on average 10 minutes has been observed centered near the equatorial regions (Figure 6). It is observed in all 6 telescopes simultaneously which is difficult to understand if the background is due to particle events as telescope pair 1 and pair 3 have look directions separated by more than 60 degrees. The magnitude of the overall enhancement varies as a function of orbital precession. It is minimized in all three telescope pair and nearly absent in telescope pair 3 which looks nearly along the spin axis just after the orbit has precessed out of the 100% sunlight condition and maximizes by the time the orbit precesses to become noon-midnight. It is often associated with bright transient events of duration <45 sec which cause FEE resets. The variability in height of the bell shaped envelope as a function of time has been studied using data from the telescopes state of health records for the 4-7 days after each full illumination of the satellite from 1993 to October of 1998. After the hot time, the background count levels are at a minimum for about two weeks From these orbits, the maximum and minimum heights of the equatorial enhancement were recorded. The maximum height observed in 1994-1995 ranged between 1000-4000 c/s then significantly decrease in 1996 time to approximately 500-1000 c/s. Currently the maximum height can exceed 20,000 c/s in 1999. The magnitude of the equatorial enhancement for telescope pair 1 is shown in Figure 7. A similar behavior is observed for the other 2 telescope pair. We believe that this variability is tied to the solar cycle, which was at a minimum in 1996 and is approaching maximum, which will occur in 2000-2001. The percentage of the sky affected by the anomalous background, however, has remained essentially the same since launch: approximately 50%.

3) Occasionally, a two minute enhancement that is often not modulated with spin period is observed at +45 and -30 degree latitude. Similar features were also observed by the gamma-ray detectors on the DMSP satellite at near the same time in 1994 at similar latitude bands and with similar duration (Klebesadel, private communication). DMSP sees these features only in the lowest energy channel (50-100 keV).

So what is this contaminating background? The pulse height distribution of this anomalous background has been analyzed and it is consistent with being photons. When the background is observed, it is also uniformly observed over the detector face. It does not appear to be associated with spacecraft vehicle glow. Neither EUVE nor the Wide Field Camera on ROSAT have reported similar behavior, but they are both primarily pointed experiments and the initial all sky surveys were performed with a much slower spacecraft rotation speed.

An unverified hypothesis to explain this phenomena involves neutral ions flowing into the telescope body through the aperture and then somehow ionizing inside the telescope body and/or ionospheric ions sweeping past the magnetic broom fields at the aperture. Since the detector filters are at the same high negative bias voltage as the front of the microchannel plates, the positive ions would be attracted to the filters and possibly cause EUV or x-ray fluorescence that would pass through the thin filters and illuminate the detectors. This hypothesis is bolstered by the observation that the anomalous background does not appear to distribute itself across the detector in the same way as the telescope vignetting function, and appears across the detector uniformly as it's rate increases, i.e. there is no evidence of an image of a boundary moving across the detector at the onset of the anomalous background.

Because the bell shaped portion of the background peaks near the equatorial region, we believe that ALEXIS provides a density probe of the Earth s upper atmosphere. The variations in the peak height as a function of solar cycle lend credence to this observation. While the peak height has changed, the percentage of sky coverage of the anomalous background as a function of solar cycle has remained unchanged, approximately 50% of the sky. The observation that the anomalous background rate in all telescopes peaks when the angle between the velocity vector and the telescope look direction reaches a value of approximately 50^{o} is puzzling.

One side effect of the anomalous background is that it causes front end electronic (FEE) resets due to the large gradients in count rates. Once an FEE reset has been initiated, data collections are stopped for the 45-90 seconds required to reset. Early in the mission, a single reset per orbit was common. Currently, however, several resets per orbit are the norm except during the days following a 100% sunlight illuminated orbit when there is still on average 1 reset per orbit. The increase frequency of resets during the remaining orbits acts to decreased even more the observing duty cycle.

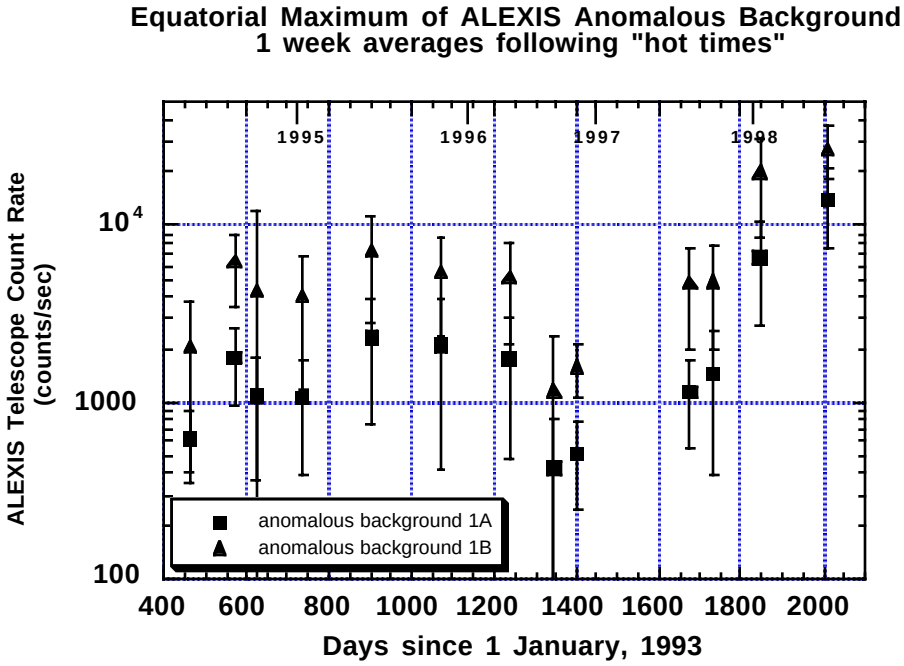

Figure 7: The observed variations in the maximum of the anomalous background observed in ALEXIS telescope pair 1. Note the minimum in 1996 that coincides with the solar minimum and the increase during 1998-1999 as solar maximum is approached.

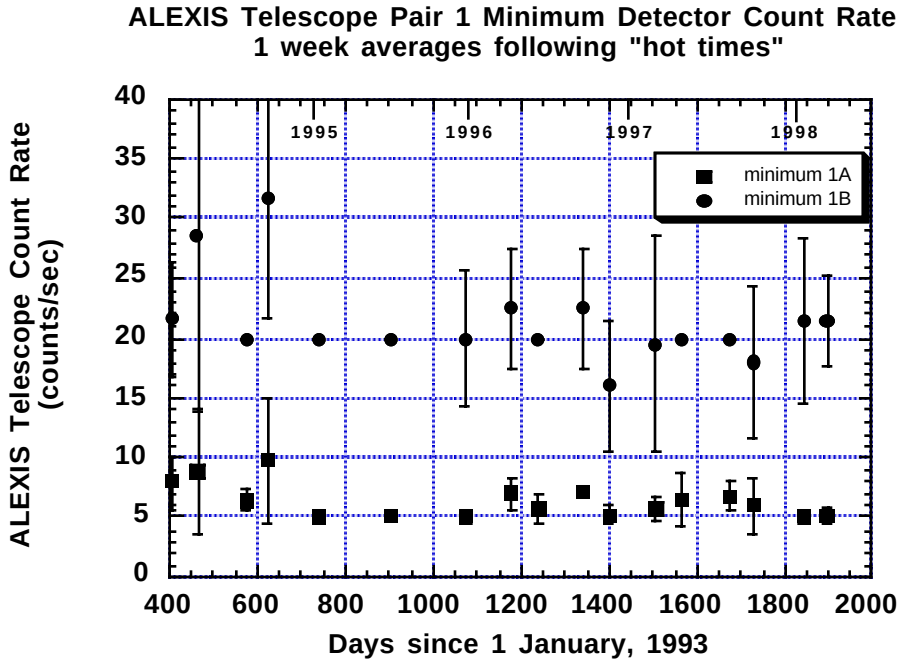

Figure 8: The telescope pair 1 count rate at the bottom of the count rate envelope as measured at the middle of the eclipse part of the orbit for the one week period after a 100% sunlight illumination orbit. The fact that these curves are so flat indicates that 1) the minimums are not affected by anomalous background and 2) the long term telescope system performance has not changed much since launch.

An extensive effort has helped to understand and characterize the ALEXIS background. This information is used by the ALEXIS telescope planners to optimize the best times to make ALEXIS observations. Originally, the telescopes were operated for up to 45 minutes per orbit which nominally included a significant portion of the auroral and polar regions. Currently, because of the degrading power system, the telescopes are operated for 25-30 minutes per orbit only between the auroral regions to maximize the best quality data.

4.2. Detector Background

Although the anomalous background observed by ALEXIS was unexpected and decreased the observing duty cycle by a factor of 2, the observed detector background is consistent with pre-flight estimates. The measurement of the bottom of what is called the "bath tub" by the ALEXIS team or the bottom envelope of the count rate distribution (see figure 6) as a function of time is displayed in Figure 8. The minimum values plotted in this figure represent the minimum of the bath tub at the middle of the eclipse. These data represent averages from the 4-7 days following a 100% sunlight illumination period from 1990 through October 1998. Data taken after a 100% sunlight illumination period, as mentioned above, is of highest quality for up to 2 weeks as the anomalous background is at a minimum. The minimum values have remained remarkably constant since launch suggesting 1) the minimums are not affected by anomalous or geocoronal backgrounds and are thus due to detector dark counts and 2) the long term telescope system performance has not changed significantly since launch from which we infer that both the filters are not oxidizing nor the mirror wavetraps degrading.

4.3. Detection of EUV Cosmic Sources

The ALEXIS flight science goals were to both detect point sources and map the EUV cosmic background. These science objectives were hampered by the delay in attitude knowledge until the attitude reconstruction algorithms were perfected[4,21]. Since successful science data processing required accurate knowledge of the satellite orientation in order to create accurate sky maps, it was several months into the mission before the first sky map was generated. The first point source detection was actually the moon in telescope pair 3 near full moon when only the spin rate was known and crude, unspun, sky plots without coordinate axis were being made. The first attitude reconstruction efforts were capable of mapping the time tagged photons back into a sky map with an accuracy of 0.5 degree. Current attitude reconstruction processing has recovered the 0.25 degree pre-flight performance accuracy.

Because the detectors can only operate during the eclipse portion of the orbit and the anomalous background obscures half the sky, the time on source averages 100-500 seconds/day. Thus, cosmic EUV sources are inherently weak (HZ 43 0.5 c/s in telescope 1B) and great care is required to extract the photon limited sources. In order to optimize point source detections, a annulus-based algorithm based upon the work of Lampton[22] was developed for use by ALEXIS. Quadrilaterilized Spherical Cube[23] sky maps are created with 0.25 degree pixels and a square kernel with a diameter of 3 pixels, and annulus of diameter of 15 pixels with a hole of diameter of 5 pixels is correlated with the sky map. The source counts are derived from the kernel radius and the background from the outer annulus. This detection method has proven to be very robust, even on portions of the sky maps where strong gradient in counts exist. Details of the point source detection effort have recently been presented by Theiler and Bloch[24,25,26].

In addition to detecting the moon and HZ 43, the ability of ALEXIS to detect EUV cosmic sources has been verified via a blind search for the brightest EUV sources detected by the EUVE satellite. In this test, one year s worth of data during 1996 was summed to generate a composite sky map and the locations of the 20 brightest EUV sources were searched for point sources. Point sources were detected within 0.3 degree of the catalog location for all of these sources.

ALEXIS is a constantly spinning satellite, and thus can monitor half the EUV sky per spin for transient sources. In order to effectively do this, 12, 24 and 48 hour summed sky maps are generated twice per day and searched for point sources. Point sources detected are compared to several star catalogs (Yale Bright Star, EUVE, ROSAT, GLEISE, Catclysmic Variable, etc) for initial source identification. Sources in excess of 4.7 standard deviations above background are sorted into known bright and unknown bright sources. Source detections above 5.2 standard deviations that are unknown trigger transient e-mail and pager alerts. As part of the pipeline processing, data is placed on the ALEXIS web site (http://alexis-www.lanl.gov/) soon after the satellite contact for use by either the LANL scientists or other observers.

ALEXIS had successfully monitored both known and unknown transient outbursts[27,28,29]. Because ALEXIS is a dedicated monitoring satellite, essentially complete outburst coverage is possible. Outbursts from known sources have been observed for the cataclysmic variables VW Hyi, AR Uma and U Gem. Several superoutbursts from VW Hyi and outbursts from U Gem have been observed. Comparison between outburst observations indicate that there can be significant differences outburst to outburst: VW Hyi peak intensities vary significantly outburst to outburst and U Gem has demonstrated both peak intensity differences as well as changes in spectral emission outburst to outburst. ALEXIS observed the brightest AR Uma EUV outburst to date in 1994 during a time of long term enhanced optical emission. A subsequent EUV outburst observed by EUVE in 1995 but not detected by ALEXIS was only accompanied by a short duration optical enhancement.

In addition to the known transient sources, it appears that ALEXIS has detected a possible new class of transient sources (false alarm rates are currently being estimated). The characteristics of this class of transient behavior is as follows: 1) outburst duration of 12-48 hours, 2) essentially uniform sky distribution, 3) transient frequency is approximately one per week, and 4) number of transients equally observed in all telescopes, but seldom detected in both coaligned telescope. Because ALEXIS has a 0.25 degree positional accuracy, it is unknown uniquely from ALEXIS observations what type of stellar system is generating the EUV emission although the sky distribution is consistent with flares from K and M type stars. In an attempt to identify the progenitors of these transients, 5 EUVE target of opportunity observations have been attempted. Unfortunately, even due to best efforts of EUVE team, by the time EUVE was able to observe the transient sources, the emission from these sources had abruptly turned off which is consistent with the initial identification with stellar flares.

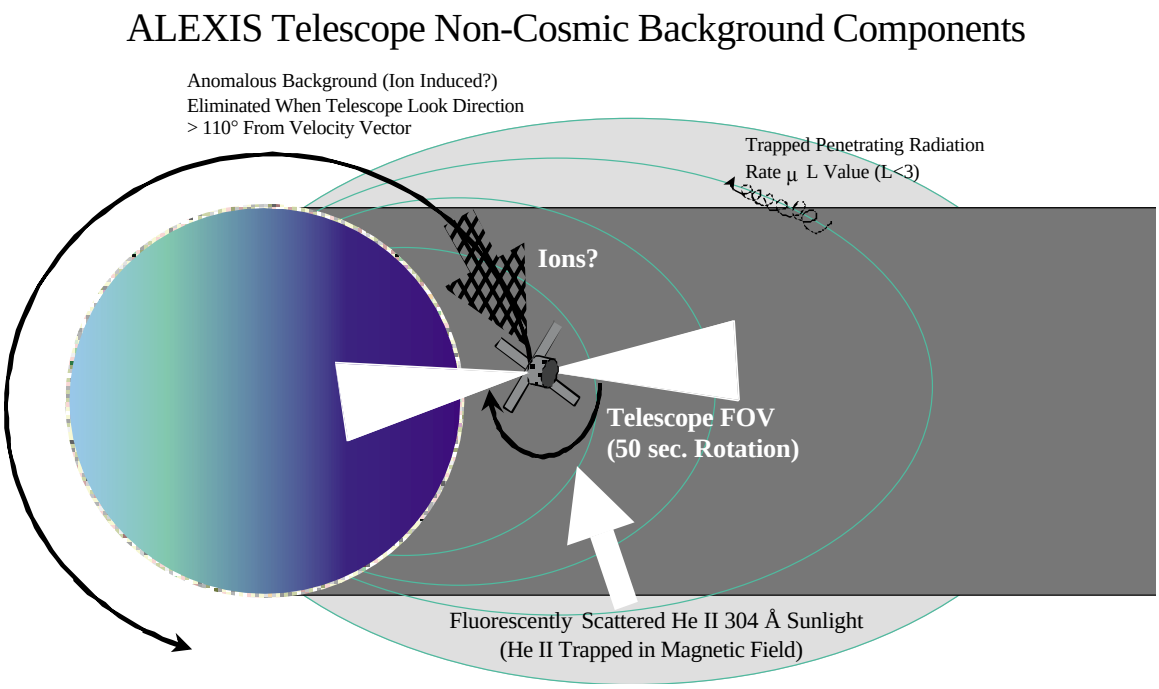

Figure 9: Several different types of backgrounds contribute to the ALEXIS count rate and therefore need to be removed in order to determine the cosmic EUV background. This figure shows the three major backgrounds that have been identified to date: 1) anomalous background, He II 304 geocoronal emission and penetrating particles that follow the geomagnetic field lines.

Extensive analysis of the multi-year count rate data from ALEXIS telescopes 1A and 1B (which scan almost perpendicular to the satellite spin axis) has yielded a qualitative model of all the ALEXIS telescope diffuse backgrounds. The various components of this background model are shown in Figure 9. These backgrounds include He II 304 geocoronal emission, penetrating particle radiation that follows the geomagnetic field line index (or "L" value), and the anomalous backgrounds reported earlier in the text. Current analysis indicates that the ALEXIS telescope 1B data shows none of the anticipated emission from the cosmic diffuse background expected from the Fe lines emitted from a million degree plasma. The original diffuse background upper limits previously reported[30] still contained some He II 304 background and as thus, overestimated the Fe line background. The new upper limits on this emission that are currently being determined are at least a factor of three to five times less than what would be predicted by models that produce the rest of the soft x-ray background measured at higher energies.

5. SUMMARY

After an initial rocky start, the ALEXIS satellite has proved to be highly successful. After more than 6 years on orbit, over all, as a system no real change in ALEXIS telescope performance has been observed. Thus, there has been no change in the filter response, the mirror reflectivity due to oxidation, or the wavetraps ability to effectively reduce the geocoronal HeII 304A background. Two telescopes have had pinholes form near the edges of the detector filters. These pinholes can be masked and removed from the processed data on the ground, but have reduced somewhat the amount of EUV data that can be acquired since they produce counts that compete for the digitizing resources.

As with all new experiments working in a new energy regime, several unexpected events were encountered. The DPU EDAC software problem was easily resolvable, so had little impact to the project. The anomalous background, on the other hand, has reduced the data acquisition ability duty cycle to 50% of original. Also, because the maximum count rate varies in sync with the solar cycle, more FEE resets have been occurring as solar maximum is approached resulting in additional losses of data.

Because of the highly inclined orbit, ALEXIS has been unable to avoid penetrating radiation. As mentioned above, the DPU EDAC problem was quickly diagnosed as being due to penetrating radiation and then a patch put in place to minimize the effects. World time averaged count rate maps have been generated which clearly show the locations of the penetrating particles and are being used to determine which parts of the orbit (latitude vs. longitude) to include data for the diffuse background studies. Because the EEPROM could be reprogrammed after more than 5 years on orbit, the total dose experience by the ALEXIS satellite is either less than the 18 month estimates from SNL as a result of flying during solar minimum or the shielding of critical components is better than originally estimated.

ALEXIS has successfully monitored both known and unknown transient outbursts. Because ALEXIS is a monitoring satellite, both more complete temporal coverage of cataclysmic variable outbursts and monitoring of the EUV sky for a new class of transient behavior has been possible. The new upper limits of the cosmic diffuse background expected from the Fe lines emitted from a million degree plasma that are currently being determined are at least a factor of three to five times less than what would be predicted by theoretical models based upon fits to the rest of the soft x-ray background measured at higher energies. This exciting new upper limit will provide an interesting challenge to diffuse background theories.

ACKNOWLEDGMENTS

ALEXIS would not have been possible without the expertise and dedication of a great many people over the past ten years since first design. This work was supported by the Department of Energy,

REFERENCES

1. W. C. Priedhorsky, et al., 1988, ALEXIS: An Ultrasoft X-Ray Monitor Experiment Using Miniature Satellite Technology , 154-164, *Proc. SPIE,* Vol. **1344** EUV, X-Ray, and Gamma-ray Instrumentation for Astronomy (1988).

2. W. C. Priedhorsky, J.J. Bloch, S.P. Wallin, W.T. Armstrong, O. H.W. Siegmund, J. Griffee and R. Fleeter, The ALEXIS Small Satellite Project: Better, Faster, Cheaper Faces Reality , *IEEE Trans. Nucl. Sci*., (1993)

3. W. C. Priedhorsky,J.J. Bloch, D.H. Holden, D.C. Roussel-Dupr , B. W. Smith, R. Dingler, R. Warner, G. Huffman, R. Miller, R. Dill, and R. Fleeter., 1993, The ALEXIS Small Satellite Project: Intiial Flight Results , 114-127, *Proc. SPIE,* Vol. **2006** EUV, X-Ray, and Gamma-ray Instrumentation for Astronomy (1993).

4. J. Bloch, T. Armstrong, B. Dingler, D. Enemark, D. Holden, C. Little, C. Munson, B. Priedhorsky, Diane Roussel-Dupre', Barry Smith, Richard Warner, Bob Dill, Greg Huffman, Frank McLoughlin, and Raymond Mills, "The ALEXIS Mission Recovery", Volume 86, *Advances in the Astronautical Sciences - 17th Annual AAS Guidance and Control Conference,* Feb 2-6, 1994, Keystone CO

5. J. J. Bloch, F. Ameduri, W. C. Priedhorsky, D. C. A. Roussel-Dupr , B. W. Smith, O. H. W. Siegmund, S. Cully, J. Warren, and G. A. Gaines, 1990, Design, Performance, and Calibration of the ALEXIS Ultrasoft X-Ray Telescopes , 154-164, *Proc. SPIE* Vol. **1344** EUV, X-Ray, and Gamma-ray Instrumentation for Astronomy (1990).

6. J. J. Bloch, W. C. Priedhorsky, D. C. A. Roussel-Dupr , B. C. Edwards, and B. W. Smith, 1992, The ALEXIS Experiment: Current Status and Performance , 83,93, *Proc SPIE,* Vol. **1743** EUV, X-Ray, and Gamma-ray Instrumentation for Astronomy III (1992).

7. D. Roussel-Dupr , J.J. Bloch, D. Ciskowski, R. Dingler, C. Little, M. Kennison, W. C. Priedhorsky, S. Ryan and R. Warner, "On-Orbit Science in a Small Package: Managing the Alexis Satellite and Experiments", *Proc. SPIE*, Vol **2267**, 76, 1994

8. D. Roussel-Dupre', J. Bloch, C. Little, R. Dingler, B. Dunne, S. Fletcher, M. Kennison, K. Ramsey, R. King, J. Theiler, J. Sutton, and J. Wren, ''ALEXIS, the little satellite that could - 4 years.'' *In Proceedings of 11th AIAA/USU Conference on Small Satellites* (1997). **SSC97-IV-3**

9. J. J. Bloch, B. Edwards, W. Priedhorsky, D. Roussel-Dupre', B. W. Smith, O. H. W. Siegmund, T. Carone, S. Cully, T. Rodriguez-Bell, J. Warren, and J. Vallerga, On Orbit Performance of the ALEXIS EUV Telescopes , *Proc. SPIE*, Vol. **2280**, EUV, X-Ray, and Gamma-ray Instrumentation for Astronomy (1994).

10. B.W. Smith, J.J. Bloch, and D. Roussel-Dupr , "Metal Multulayers for EUV Wide Field Telescopes", *Optical Engineering*, Vol **29**, No 6, page 592, 1990.

11. M. Born and E. Wolf, *Principles of Optics*, Pergamon Press, London, 1959.

12. D. L. Windt, Thesis, U. Colorado, 1987.

13. E. B. Palik, *Handbook of Optical Constants*, Academic Press, New York, 1985.

14. H.J. Hagemann, W. Gudat, C. Kunz, "Optical Constants from the Infrared to the X-ray Region: Mg, Al, Cu, Ag, Au, C Al_2O_3.", *DESY Report SR-74/7*, Hamburg, 1974.

15. J. Bloch, B.W. Smith, and D. Roussel-Dupre', U.S. Patent #5086443, Background Reducing Multilayer Mirrors

16. D. Roussel-Dupre' and F. Ameduri, ''Uniformity results of the multilayer mirrors used in the ALEXIS ultrasoft X-ray telescopes.'',. *Proc. SPIE*, Vol **1742**, 621-629 (1993).

17. O. H. Siegmund, S. Cully, J. Warren, G. A. Gaines, W. Priedhorsky, and J. Bloch, Highly Curved Microchannel Plates , *Proc. SPIE*, Vol **1344**, p. 346-354 (1990)

18. S. Starin, D. Roussel-Dupr and J. Bloch, Flight performance of UV filters on the ALEXIS satellite , *Proc. SPIE*, Vol **3765** (1999)

19. J. Bloch, B. Edwards, W. Priedhorsky, T. E. Pfafman, D. Roussel-Dupre', B.W. Smith, The ALEXIS EUV Sky Monitor and Survey Experiment: Design, Pre-flight Calibration, and In-Orbit Performance , in progress

20. D. Roussel-Dupr , and J. J.Bloch, "The Anomalous Background Observed by the ALEXIS Telescopes", Workshop on the Earth's Trapped Particle Environment, 1996, p 193, Editor G. Reeves, *AIP Conference Proceedings 383*

21. M. L. Psiaki, J. Theiler, J. Bloch, S. Ryan, R. W. Dill, and R. E. Warner, ''ALEXIS spacecraft attitude reconstruction with thermal/flexible motions due to launch damage.'' *Journal of Guidance, Control, and Dynamics* **20**, 1033-1041 (1997).

22. M. Lampton, Two-sample discrimination of Poisson means , *Astrophysical Journal*, Part 1, vol. **436**, no. 2, December 1, 1994, p. 784- 786

23. E. W. Greisen and M. Calabretta, Representations of Celestial Coordinates in FITS , Astronomical Data Analysis Software and Systems IV, ASP Conference Series, Vol. 77, 1995, R.A. Shaw, H.E. Payne, and J.J.E. Hayes, eds., p. 233.

24. J. Theiler and J. Bloch, "Heuristic estimates of weighted binomial statistics for use in detecting rare point source transients", in Astronomical Data Analysis Software and Systems VI, vol. **125** *of Astronomical Society of the Pacific Conference Series*, G. Hunt and H. E. Payne, eds., pp. 151-154. (1997)

25. J. Theiler and J. Bloch, "Nested Test for Point Sources", in Statistical Challenges in Modern Astronomy II, G. J. Babu and E. D. Feigelson, eds. (Springer Verlag, New York, 1997), pp. 407-408. (1997)

26. J. Theiler and J. Bloch, Multiple Concentric Annuli for Characterizing Spatially Nonuniform Backgrounds , *Astrophysical Journal*, July 1, 1999, Vol. **519**

27. D. Roussel-Dupre', J. Bloch, J. Theiler, T. Pfafman, and B. Beauchesne, "Detecting EUV Transients in Near Real Time with ALEXIS, in Astronomical Data Analysis Software and Systems" V, G. H. Jacoby and J. Barnes, eds., vol **101** of *Astronomical Society of the Pacific Conference Series*, pp. 112-115. (1996)

28. D. Roussel-Dupre', T. Pfafman, J. Bloch, and J. Theiler, ''EUV sources and transients detected by the ALEXIS satellite.'' InMultiwavelength Astrophysics. Vol. **179** of *IAU Colloquium Series* (1996).

29. D. Roussel-Dupre', J. Bloch, S. Ryan, B. Edwards, T. Pfafman, K. Ramsey, and S. Stem, ''The ALEXIS point source detection effort.''In Astrophysics in the Extreme Ultraviolet, S. Bowyer and. F. Malina, eds. Vol. **152** *of IAU Colloquium Series* (Kluwer Academic, Dordrecht,), pp. 485-490 (1996)

30. B. W. Smith, T. E. Pfafman, J. J. Bloch, and B. C. Edwards, ''ALEXIS observations of the diffuse cosmic background in the extreme ultraviolet.'' InAstrophysics in the Extreme Ultraviolet, S. Bowyer and R. F. Malina, eds. Vol. **152** *of IAU Colloquium Series* (Kluwer Academic, Dordrecht, 1996), pp. 283-287.